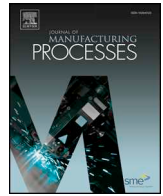# Investigation of micro-textured cutting tools used for face turning of alloy 718 with high-pressure cooling

N.B. When citing this work, cite the original published paper.

(article starts on next page)

Investigation of micro-textured cutting tools used for face turning of alloy 718 with high-pressure cooling

Nageswaran Tamil Alagan[a,*], Pavel Zeman[b], Philipp Hoier[c], Tomas Beno[a], Uta Klement[c]

[a] Department of Engineering Science, University West, Trollhättan, Sweden
[b] Research Center of Manufacturing Technology, Czech Technical University in Prague, Prague, Czech Republic
[c] Department of Industrial and Materials Science, Chalmers University of Technology, Gothenburg, Sweden

ARTICLE INFO

ABSTRACT

There is an increasing demand to improve the service life of cutting tools during machining of heat resistant superalloys (HRSA). Various studies showed that textured cutting tools improved the tribological properties and reduced cutting forces, temperature, and tool wear. Surface texturing can be seen as a futuristic design to improve the performance of the cutting tool and to increase productivity. However, only limited research has been conducted in machining superalloys with textured inserts and high-pressure coolant. In this work, three different micro texture designs on both rake and flank face are investigated in combination with high-pressure coolant in machining Alloy 718. Due to better tool life predictability, carbide cutting tools are used in machining components made from superalloys. However, the disadvantage is that machining can only be done at lower cutting speed/feed rate/depth of cut with high tool wear rates. The experimental investigation using different tool wear analysis methods showed that the combination of a cylindrical dimple on the rake and the square pyramid texture on the flank surface improved the wear resistance of the tool. An increase in tool life of about 30% was achieved as compared with a regular insert for the investigated cutting conditions. Different levels of adhering workpiece material were observed on the rake face of textured tools. Furthermore, the chip backside showed imprints from the tool textures. The tool textures on the rake face have influenced the tool-chip friction conditions during cutting.

1. Introduction

Alloy 718 is a nickel base material with high mechanical and thermal strength at elevated temperature. Therefore, it is frequently used in the hot zones of the jet engines such as the combustion chamber and the turbine. Additionally, Alloy 718 has good weldability and creep resistance at elevated temperatures, which makes it a suitable choice for fabrication of jet engine components. For instance, Alloy 718 components account for 50% of overall superalloys used in some Pratt and Whitney engines [1]. However, when it comes to machining, Alloy 718 shows poor machinability mainly due to its low thermal diffusivity, the presence of hard abrasive phases, and its ability to work harden and to retain hardness and strength at higher temperature [2]. Therefore, during machining, the workpiece material acts as a thermal insulator on the cutting edge, which leads to the increase in the steady-state temperature in the cutting zone. Consequently, lowering the service life of the tool [3].

Despite the current machining technology and available cooling strategies, heat dissipation from the cutting zones during machining of Alloy 718 and other heat resistant superalloys is still challenging. One of the solutions to improve the heat dissipation from the cutting zone was to focus a high-pressure coolant jet to the cutting edge. In 1952, Pigott and Colwell [4] built a high-pressure system able to deliver the coolant at a maximum pressure of 4 MPa, which led to increase in tool life by 7–8 times. Since then, high-pressure coolant technology was widely used in the metal cutting industry to improve tool life and surface quality, and to achieve high productivity.

Recently, there has also been considerable attention to the influence of the textured cutting tools in combination with conventional cooling for improving tribological properties between the contact surfaces. The studies on machining different workpiece material types revealed that textured cutting tools have the potential to effectively improve the machinability of the respective alloys by significantly reducing cutting forces and temperatures as well as friction and material transfer to the tool surfaces. Furthermore, texturing of tools has shown to have a beneficial influence on chip formation [5–11].

For instance, Kawasegi et al. [5] investigated micro and nano scale textures on a WC-Co cutting tool surface using femtosecond laser with the aim of controlling the tribological characteristic of the tool. The textured WC-Co tools were used in turning of an aluminium alloy with minimum quantity lubrication. As reported by the authors, the textured tools lowered the cutting forces when the cutting speed was higher than 420 m/min. Friction in the secondary shear zone was reduced by having textures perpendicular to the chip flow. This showed that textured cutting tools effectively improved the machinability of the aluminium alloy.

Lei et al. [6] conducted experiments on mild steel by investigating the performance of a lubricated array of microholes in the surface of WC-Co inserts. To have them act as micropools, solid and liquid lubricants such as tungsten disulfide and oil were used to fill the microholes. As reported by the authors, the textured tools reduced the mean cutting forces by 10–30% and tool-chip contact length by 30%. Non-textured tools formed straight and long chips, while textured tools produced coiled chips. With respect to lubrication, both solid and liquid lubricants were equally effective in reducing the contact length and friction coefficient at the tool-chip interface.

Enomoto et al. [7] used face milling and TiAlN coated tools with a periodically stripe-grooved surface to reduce tool wear when machining steel. Tools with nano/micro grooves (100–150 nm deep and 700 nm apart) did not improve the wear resistance. However, micro-stripe grooves (5 mm deep, 20 mm wide and 20 mm apart) parallel to the main cutting edge of the TiAlN coating significantly improved the wear resistance and lubricity on the rake surface.

The experimental results of Kawasegi et al. [5], Sugihara and Enomoto [8] and Obikawa et al. [9], showed that micro textures reduced the cutting forces, when fabricated parallel and continuous (grooves) to the cutting edge on the rake face compared to the perpendicular position and discontinuous texture (pits). In contrast, Koshy and Tovey [10] reported that areal textured cutting tools showed a better performance in terms of lower cutting forces than the linear texture when machining steel and aluminium alloys. The investigation of textured tool performance was extended to the titanium alloy Ti-6Al-4V by Ma et al. [11]. They performed 3D numerical simulations with respect to the performance of microgrooves on the rake of WC cutting tools in dry turning. Microgroove parameters such as width, depth and distance from the cutting edge were investigated. Their results showed that the micro grooved cutting tools effectively reduced the cutting forces and the frictional behaviour of the tool-chip interface.

Overall results have shown that both the application of high-pressure coolant and surface textured cutting tools (either on rake or flank) can be beneficial for enhanced tool life and surface quality of the machined part. The combination of both technologies is therefore considered to be a promising approach for enhanced interaction of the coolant and the cutting tool. This is of particular interest for difficult to machine materials such as heat resistant superalloys.

So far, only Fang and Obikawa [12] investigated five different textures on the flank face of the tool when machining Alloy 718 with a

Table 1
Insert nomenclature and cutting edge geometry specification.

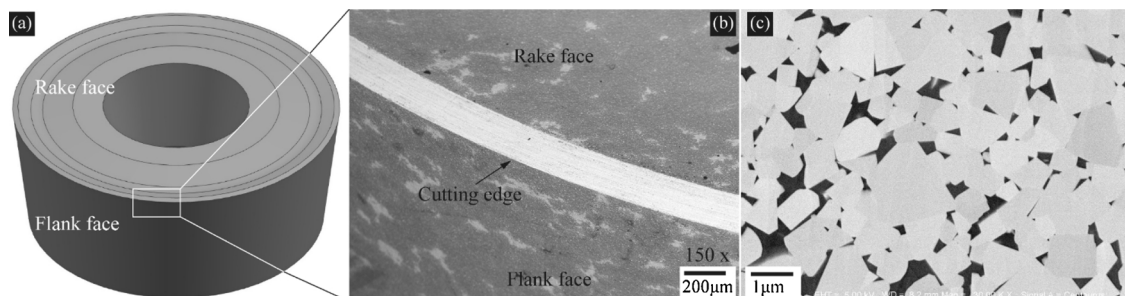| Insert	Regular
	Gen 0/G 0
	Gen I/G I
	Gen I+/G I+
Insert shape	Round
Type of insert	Uncoated carbide insert
Insert thickness [mm]	4.76
Inscribed circle diameter [mm]	12
Face land length [mm]	0.2
Face land angle [°]	−17
Rake angle [°]	12
Clearance angle [°]	7
Cutting edge radius [mm]	0.005

flank-sided coolant supply pressure of 13 MPa. Their results showed that textures enhanced the heat transfer from the tool to the coolant. In addition, flank and crater wear decreased compared to the non-textured tool. The rate of tool wear on the textured tool was related to the array and depth of the texture. Temperature measurements using thermocouples and EDS results showed an improved cooling performance of the textured tool.

However, despite its obvious potential, there is not much research done on combining high-pressure coolant supply with surface texturing of cutting tools. In particular, the simultaneous application of high-pressure coolant and texturing on both rake and flank of the tool has not been studied. Hence, the aim of this research work was to investigate how different tool textures combined with high-pressure coolant on both rake and flank can influence the obtained tool wear and tool-chip contact conditions when machining Alloy 718. Additionally, the influence of rake textures on the chip formation was investigated. The obtained results on tool wear are compared with those of regular, conventionally available inserts and reasons for the obtained differences are discussed in the following sections.

2. Surface feature on regular insert

2.1. Regular insert description

A commercially available regular insert round insert with ISO nomenclature RCMX 12 04 00 (Grade H13A) was used as the reference. This grade is recommended for machining Ni-based superalloys when high bulk toughness is required. Moreover, round inserts have high edge strength and are therefore preferably used in roughing operations [13]. A regular insert was laser textured to the desired design of Gen 0, Gen I, and Gen I+ described in detail in subsections 2.2–2.4. Nomenclature as well as cutting edge geometry specification of the RCMX insert is provided in Table 1. The insert is made of uncoated sintered carbide ; consisting of 95% tungsten carbide (WC) and 5% cobalt (Co) binder. Illustrations of the insert and of the WC-Co microstructure are provided in Fig. 1. The sharp-edged WC grains are uniformly

Fig. 1. (a) Illustration of the regular insert; (b) magnified SEM micrograph of the cutting edge, and (c) microstructure of the H13A sintered carbide tool (WC particles are bright and the Co-binder is the dark phase).
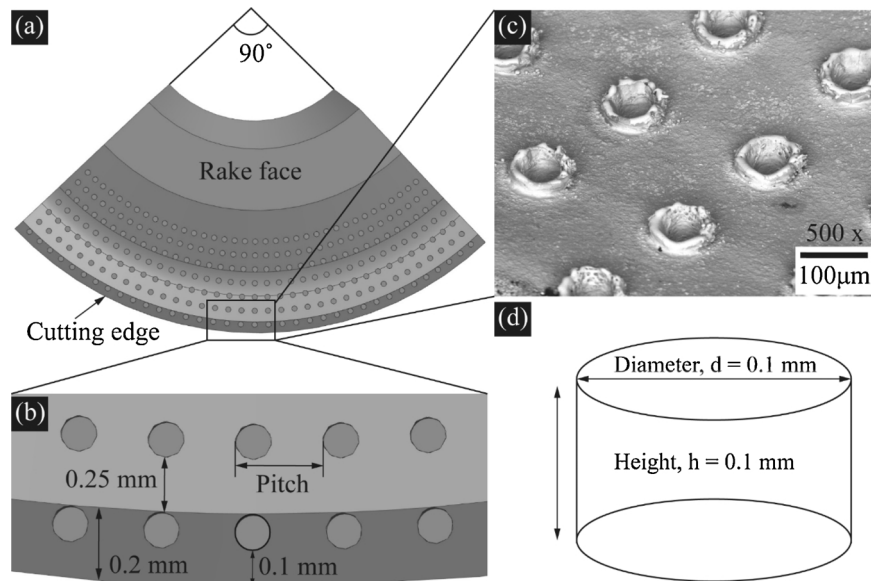
Fig. 2. (a) Illustration of the Gen 0 insert; (b) the detailed illustration of a rake face structure; (c) magnified SEM micrograph of the rake face, and (d) cylindrical element of the structure with dimensions.

distributed and have an average diameter and area of 0.65 μm and 0.45 μm^2, respectively. The insert had a hardness of 1545 ± 14 HV 30. To ensure consistency of tool geometries for the cutting tests, all inserts were inspected for face land length (Fig. 1(b)).

2.2. Gen 0

A regular insert was textured on the rake face by laser ablation method. Cylindrical dimple shapes were placed perpendicular to the surface and in a periodic array of seven rows. This textured insert is named Gen 0 insert and the design is illustrated in Fig. 2. Gen 0 structures were created using a pulsed Nd-YAG laser, LASER diode LD50C, operated at 1064 nm. Optimized laser pulse parameters were used as follows: pulse duration of 120 ns; frequency of 2.5 kHz; engraving time of 10 ms, laser spot size of 100 μm with output power of 15 W. Seven rows of dimple textures were generated parallel to the cutting edge. The distance between each row is 0.25 mm, which is a constant value. The pitch is of 0.25 mm for the first row close to the cutting edge, see Fig. 2(b), the pitch value decreases for the rows closer to the centre of the insert, due to the geometry of the insert. The position of the first row of dimples was placed on the facet and 0.1 mm away from the cutting edge as shown in the Fig. 2(b). Every cylindrical dimple was designed for a diameter and depth of 0.1 mm, see Fig. 2(d). Based on the preliminary optimization experiments, the dimple diameter, pitch and position from the cutting edge were chosen. The Gen 0 design has no negative effect on the structural integrity of the cutting tool. The real diameter of the dimple was measured as 0.078 mm in average. This is caused by the Gaussian mode of power density

distribution in the laser beam and by the selected strategy for manufacturing of the dimples. The function of this structure relies on several fundamental interacting phenomena. The concept is based on the fact that this type of surface texturing changes the friction conditions at the tool-chip interface. Laser-created dimples in contact with the chip are filled with workpiece material during machining. Alloy 718 has significantly lower thermal conductivity (k = 11.2 W/m/K) than the used sintered carbide (approx. k = 80 W/m/K). The tool removes less heat from the cutting zone when the dimples are filled with the work material. Hence, the heat transferred to the tool decreases, which results in, lowering of the tool wear rates. The chip velocity can decrease owing to an increased adhesion between chip and tool rake face. Higher adhesion can be caused by the rough surface of the rake face as well as by sticking of chip and workpiece material in the dimples. This effect can be increased by placing the first row of dimples directly on the facet. The remaining dimple structure can sustain improved heat dissipation by the coolant.

2.3. Gen I

The Gen I insert was designed to have an increase in surface area compared to the regular insert to influence the heat dissipation rate from the hot areas of the insert, Fig. 3(a–c). A square pyramidal structure was chosen as texture geometry as it creates the highest increase in the surface area for the constant volume removed. Using a standard nano-second pulse fiber laser with a 20 W source and the smallest laser spot size of 40 μm, regular inserts were textured by laser ablation at a sector of 90° on the rake and the flank face. Square
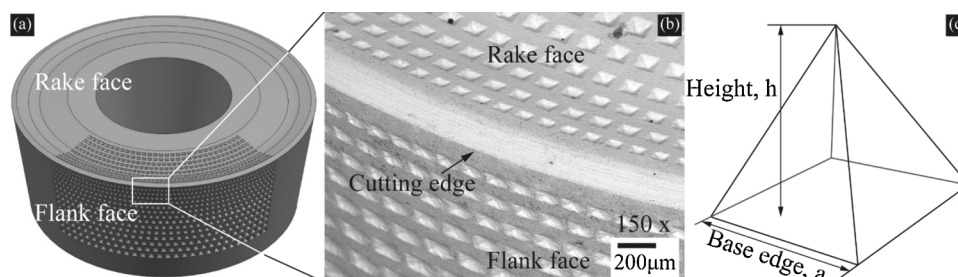
Fig. 3. (a) Illustration of the Gen I insert; (b) magnified SEM micrograph of the cutting edge showing the pyramidal textures on flank and rake face; and (c) sketch of the square pyramid texture.
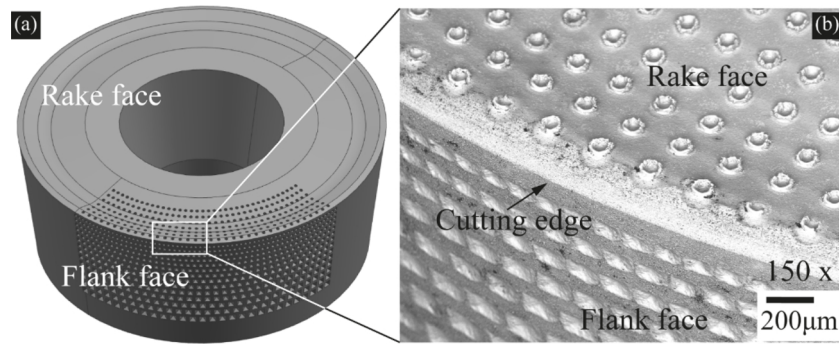
Fig. 4. (a) Illustration of the Gen I+ insert; and (b) SEM micrograph of the insert at the cutting edge.

pyramid geometry has led to an increase of the surface area by approx. 5.6 times. A more detailed description of the Gen I insert design is provided by Tamil Alagan et al. [14].

2.4. Gen I+

The Gen I+ insert is shown in Fig. 4. It is a combination of the structures, principles and laser texturing of Gen 0 and Gen I. For this insert type, dimples were created on the rake face and pyramids on the flank face. Rake and flank face structures were of the same dimensions as for Gen 0 and Gen I, respectively. The aim of combining these two designs was to have better effect by influencing tool-chip contact area with Gen 0 design and increased surface area on the flank by Gen I design. Thus, in combination with the high-pressure coolant, this should improve the heat dissipation from the shear zones.

3. Experimentals

Face turning of cast Alloy 718 (average hardness of 381 ± 21.8 HV) was conducted in a 5-axis CNC machine as shown in Fig. 5(a). The hardness of the machined workpiece was measured on polished cross sectional samples using a Vickers diamond indenter applying a test force of 10 kgf. The obtained average hardness comprises 40 randomly distributed indents throughout the whole cross section of the workpiece ring. High-pressure coolant was supplied to both rake and flank face through a specially designed tool holder for the precise focus of the coolant to the cutting edge, see Fig. 5(b). The rake nozzle impact points and angle between them are illustrated in detail in Fig. 5(c). An emulsion concentration of 5% mixed with water was used as coolant, which is a recommended ratio by the coolant producer. Coolant was supplied to the rake using a pressure of 16 MPa through three nozzles with a diameter of 0.8 mm and a flow rate of approx. 11 l/min. The coolant supply pressure to the flank was 8 MPa through two nozzles with a diameter of 1.2 mm and a flow rate of approx. 12 l/min [14].

The dimensions of the Alloy 718 ring are illustrated in Fig. 6(a) and (b). The machined length in radial direction was approx. 8 mm. The corresponding spiral cutting length, SCL, was calculated from Eq. (1). The experimental setup and a SCL of 60 m were kept constant during the facing operations.
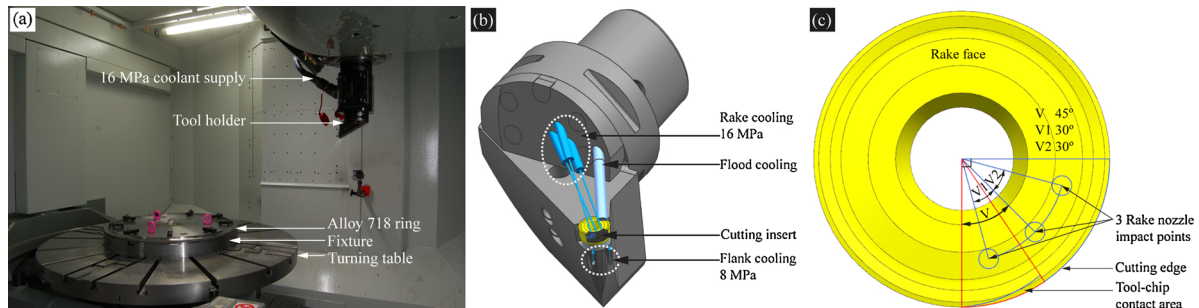

Fig. 5. (a) Experimental setup of 5 axis machine; (b) Special designed high-pressure coolant tool holder with three nozzles directed to rake and two nozzles to flank extracted from [14]; (c) Impact points of three nozzles on the rake face.
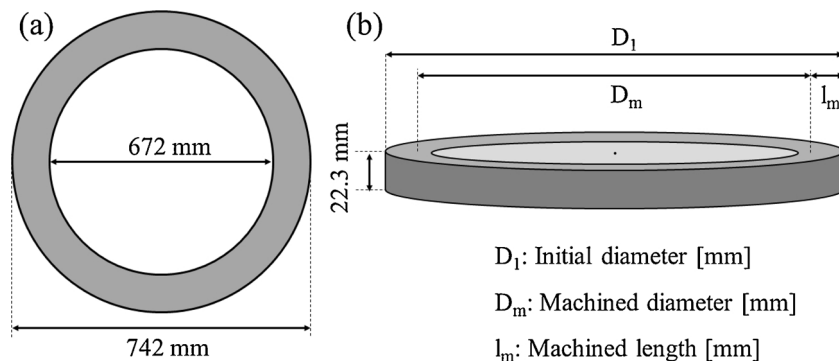

Fig. 6. (a) Top view (b) Side view of the ring with dimensions extracted from [14].

Table 2
Cutting parameters for facing operation of Alloy 718.

S.no	SCL [m]	a_P [mm]	v_c [m/min]	f_n [mm/rev]	Rake Pressure [MPa]	Flank Pressure [MPa]	Insert
1	60	1	60	0.3	16	8	Regular
2	60	1	60	0.3	16	8	Gen 0
3	60	1	60	0.3	16	8	Gen I
4	60	1	60	0.3	16	8	Gen I+

$$SCL = \left[\frac{D_1 + D_m}{2} \right] \times \left[\frac{\pi}{1000} \right] \times \left[\frac{l_m}{f_n} \right] \tag{1}$$

The cutting conditions, v_c = 60 m/min, f_n = 0.3 mm/rev, a_p = 1 mm, rake pressure of 16 MPa, flank pressure of 8 MPa, and SCL of 60 m were kept constant for all tests. A constant feed rate of 0.3 mm/rev was chosen because of the texture position on the rake face as a lower feed rate would not create contact with the texture. For each test, the cutting time was about one minute. Cutting conditions were kept constant based on the research methodology of varying one parameter and in this investigation, the cutting tools with different textures were tested. As shown in Table 2, four different tools were used for each experimental machining condition. Moreover, each condition was repeated at least two times, to ensure the repeatability. The experiments were conducted in randomized order to avoid systematic errors.

Tool wear investigations were performed on all the inserts after machining using different techniques. Light optical microscopy, LOM, and scanning electron microscope, SEM, were used to measure and examine the flank wear and wear mechanisms. 3-D scanning based on focus variation was used to scan and measure the flank wear area, tool-chip contact area, and for performing volume difference measurements. Energy dispersive X-ray spectroscopy, EDX, was used to perform chemical analysis. The measurement of average width, VB, and maximum width, VB_{max}, of the flank wear land was conducted based on the ISO 1993:3685 standard [15]. In addition, the total flank wear area, VB_{area}, was measured for precise evaluation of the flank wear for the conducted tests, see Fig. 7(a). Tool-chip contact areas were measured based on the contact angle of 34° on the rake face, see Fig. 7(b). Chip thickness measurement was carried out using the device with measurement gauge Mitutoyo 243-250B (accuracy of 3 μm). Due to the point measurement technique, the chip thickness measurement is not influenced by the curvature of the chip. In total, five chips were chosen for every cutting

Fig. 7. Evaluation of tool wear: (a) flank face with indication of area of flank wear land (VB_{area}) and maximum width of flank wear land (VB_{max}); (b) rake face with an indication of the tool-chip contact area.

condition and measured three times at different positions of the chip. This procedure was carried out for all the experimental conditions.

4. Tool wear investigations

4.1. Flank wear

Flank wear occurs due to abrasion of tool material during contact with the workpiece while cutting. The width of the wear land is usually used to determine the service life of the tool. Fig. 8 shows the flank wear lands for the four different cutting tools after the face turning test. The highest flank wear was observed for the regular insert and the lowest for Gen I+ cutting tools. The Gen I+ insert lowered the maximum and average flank wear by approx. 31% and 21%, respectively, compared to the regular insert. The results were plotted in Fig. 9(a) and showed significant standard deviations for all the tests. As seen in Fig. 8, all tools had their maximum flank wear in the leading part of the tool cutting edge where the highest chip thickness occurs during cutting.

For further analysis, flank wear area measurements were conducted using 3-D measurements. The results are plotted in Fig. 9(b). The robustness of the measurement in terms of area lowered the standard deviation bar. The results showed that the Gen I+ inserts reduced the flank wear area by approx. 30% as compared to the regular insert. This can be attributed to the increased surface area on the flank face, which led to improved heat dissipation by creating access for the high-pressure coolant to get closer to the cutting edge. Increase in heat dissipation and penetration of cutting fluid to the cutting zone helps to protect the tool from reaching thermal decomposition temperature. Although the Gen 0 insert only had textures on the rake face, it decreased flank wear area approx. by 22%. This can be due to the change in the sticking and sliding condition in the rake face influencing the chip formation. The overall flank wear land observation showed that the textured tools in combination with high-pressure coolant had less wear land than the regular insert. Fang and Obikawa [12] and Jäger et al. [16] reported similar observations of reduced flank wear and movement of the coolant precipitates due to an improved heat dissipation rate.

4.2. Tool-Chip contact area

The tribological contact between the tool and chip in the secondary shear zone influences chip formation and tool wear. In this zone, chips undergo high stress and strain due to the friction, which leads to an increase in the cutting temperature and the tool wear rate. Measurement of tool-chip contact is of vital interest to understand the effect of textures on the rake face of the tools in influencing the tool-chip contact zone and the wear mechanism. It should be noted that the round shape of the cutting tool could influence the measurement of the contact length. Therefore, a set of guidelines was taken into consideration based on the contact angle in measuring tool-chip contact area; see Fig. 7(b). The theoretical chip contact area for Gen I and Gen I + inserts are shown for feed rate 0.3 mm/rev in Fig. 10.

A 3-D focus variation microscope was used to measure the tool-chip contact area for the four cutting tools and their corresponding replicates. The average tool-chip contact area with standard deviations are shown in Fig. 11. As can be seen, the textured tools are not affecting the contact area. The selected tools were closely examined with SEM. Interestingly, the observed wear and adhesion phenomena were different for Gen 0 and Gen I+ inserts compared to the regular and Gen I inserts.

The SEM micrographs for four selected tool rake faces are shown in Fig. 12(a–h). All the tools were found to have significant adherence of workpiece material on the rake face. The regular insert in Fig. 12(a–b) showed the traces of the coolant precipitate as a dark region between tungsten carbide close to the tool-chip contact zone. Similar findings of eroded cobalt from the flank face due to coolant boiling in the region
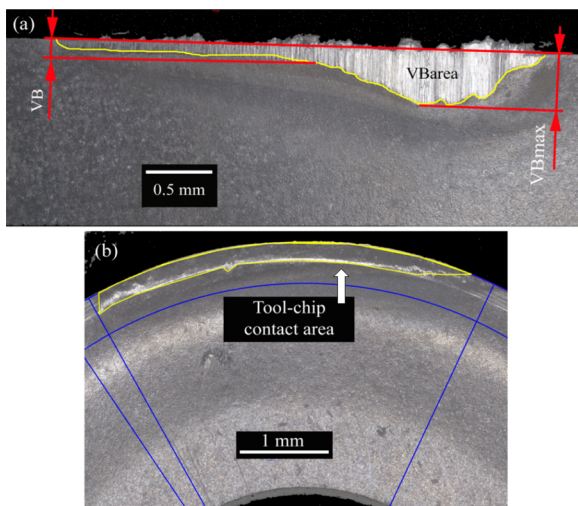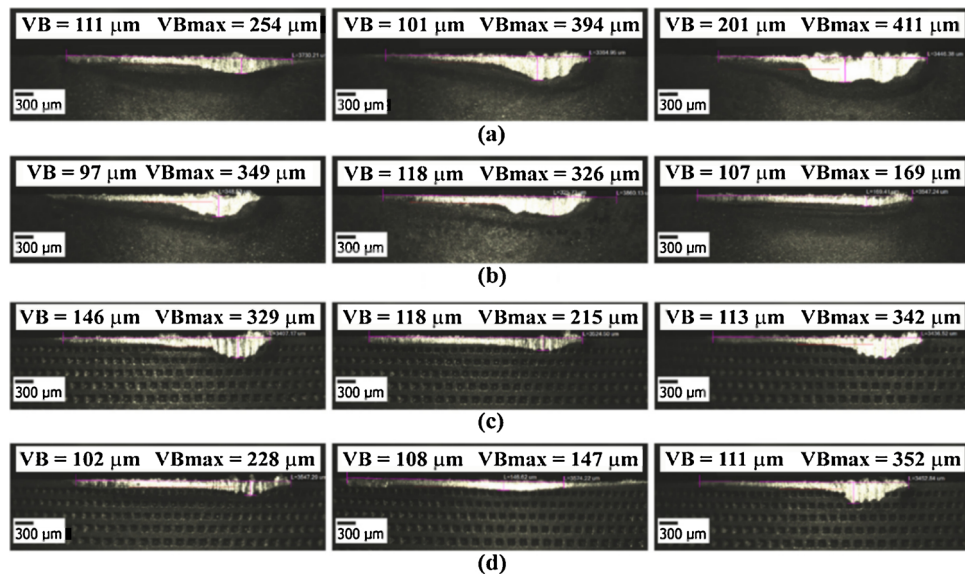
Fig. 8. Flank wear land of inserts (a) regular, (b) Gen 0, (c) Gen I, and (d) Gen I+.
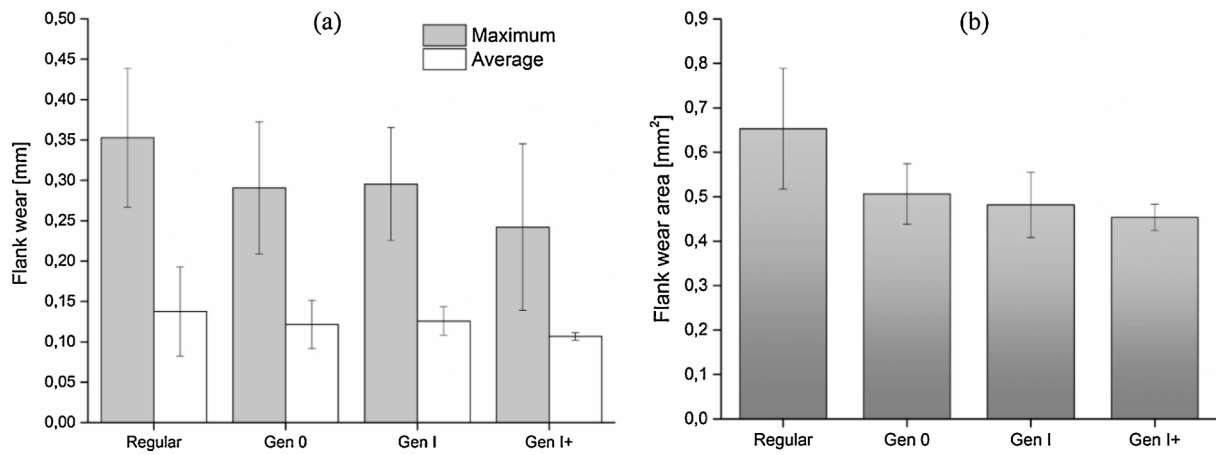

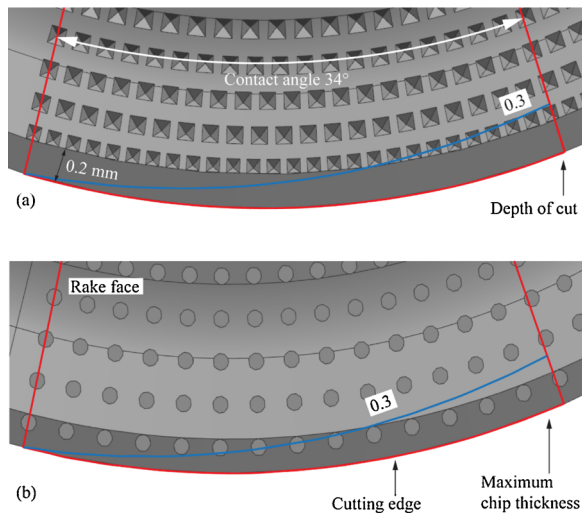**Fig. 9.** Comparison of (a) average and maximum measured flank wear and (b) flank wear area.

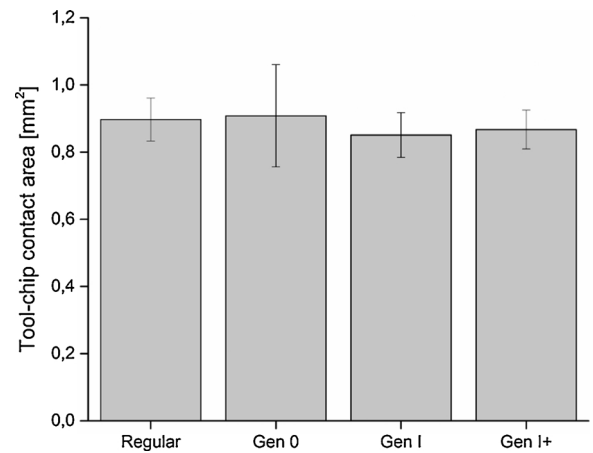**Fig. 10.** Theoretical chip contact area (a) Gen I and (b) Gen I+ insert for feed rate 0.3 mm/rev.
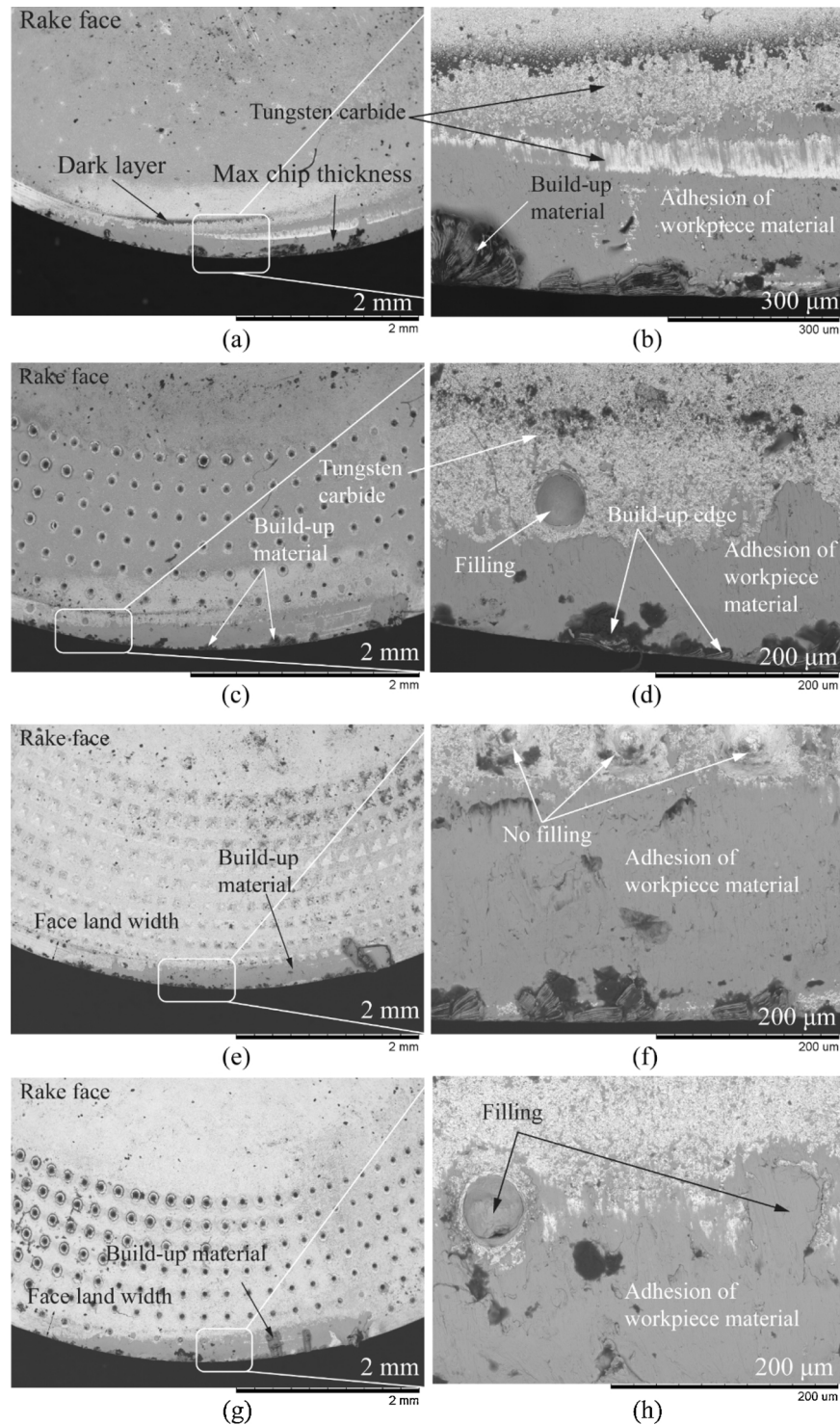

Fig. 11. Tool-chip contact area measurement.

was found by Hoier et al. [17]. In the case of Gen 0 and Gen I+ inserts, the textures close to the cutting edge were filled with workpiece material, Fig. 12(d) and (h). With respect to friction and sliding

Fig. 12. Rake face of the inserts examined in SEM after machining: (a–b) regular insert; (c–d) Gen 0 insert; (e–f) Gen I insert; (g–h) Gen I+ insert. Adhesion of workpiece material seen as light grey colour and build-up-edges/material seen in dark colour, tungsten carbide is visible in white colour.

mechanism between the chip and textured tools, Gen 0 and Gen I+ were probably different compared to the regular and Gen I tool. In case of the Gen I insert, no filling of workpiece material was observed due to the position of the texture 0.2 mm from the cutting edge. Although the tool-chip contact areas were similar, the maximum flank wear and flank wear areas were lowered by approx. 30% for Gen I+ inserts compared to other tools, see Figs. 8(d) and 9. Therefore, the textures are important in the secondary shear zone and need to be placed close to the cutting edge, which can decrease the tool wear.

4.3. Material adhesion

The tilted view of one of each tool type's cutting edges after the machining tests are shown in Fig. 13, focussed on the areas of maximum chip thickness and maximum flank wear. SEM images (left column) show that independently of the tool type, the flank wear lands as well as the areas of chip contact on the rake faces are subjected to adhesion of the workpiece material (dark). The 3D topography scans in the right column of Fig. 13 show a negative geometrical deviation on the flank

faces, which can be connected to the tool material loss due to the flank wear. No signs of substantial crater wear can be seen. Instead, positive geometrical deviations can be observed as a result of comparably thick adhesion layers on the rake faces of all inserts. Furthermore, no major changes of the cutting edges' geometries due to chipping or substantial plastic deformation can be seen.

As evident in Fig. 13(c–h), the chip-rake contact zone stretches into the patterns present on the rake sides of all the modified inserts. Higher magnified views of the first rows of rake patterns of a Gen I+ and Gen I insert are shown in Fig. 14(a) and (b), respectively. The first row of patterns in Fig. 14(a) is partially filled with workpiece material, whereas the second row is adhesion free. In Fig. 14(b), however, the first row of the indents is not filled with workpiece material. This is due to the longer distance of the indents from the cutting edge as compared to Gen I+. Instead, the adhesion is present on the sides of the indents.

In addition to the adhesion of Alloy 718 to the tool-workpiece

contact areas on rake and flank, the SEM investigation revealed adhesion layers outside these areas where no tool-workpiece contact occurs during machining. Examples are given in Fig. 15(a) and (b) where SEM images of the worn cutting edges of Gen I+ inserts are shown. As can be seen, areas just below the flank wear land and the first row of indents appear black. Similar black layers were found on flank faces of all inserts after the machining tests, irrespective of tool modification. For further investigation of these zones, EDX analysis was conducted.

Dark regions observed below the flank wear of the Gen I+ tool, see Fig. 15a, were identified to be precipitates originating from the coolant. EDX analysis obtained on a dark adhesion layer of a regular insert is provided in Fig. 15c. Accordingly, the dark layers comprise mostly of C, Nb, S, O and Ca. Note that the peaks of W and Co are likely to originate from the underlying tool material and are not belonging to the dark layer. Presence of elements of the tool material in the spectrum furthermore suggests that the dark layer is thinner than the generation
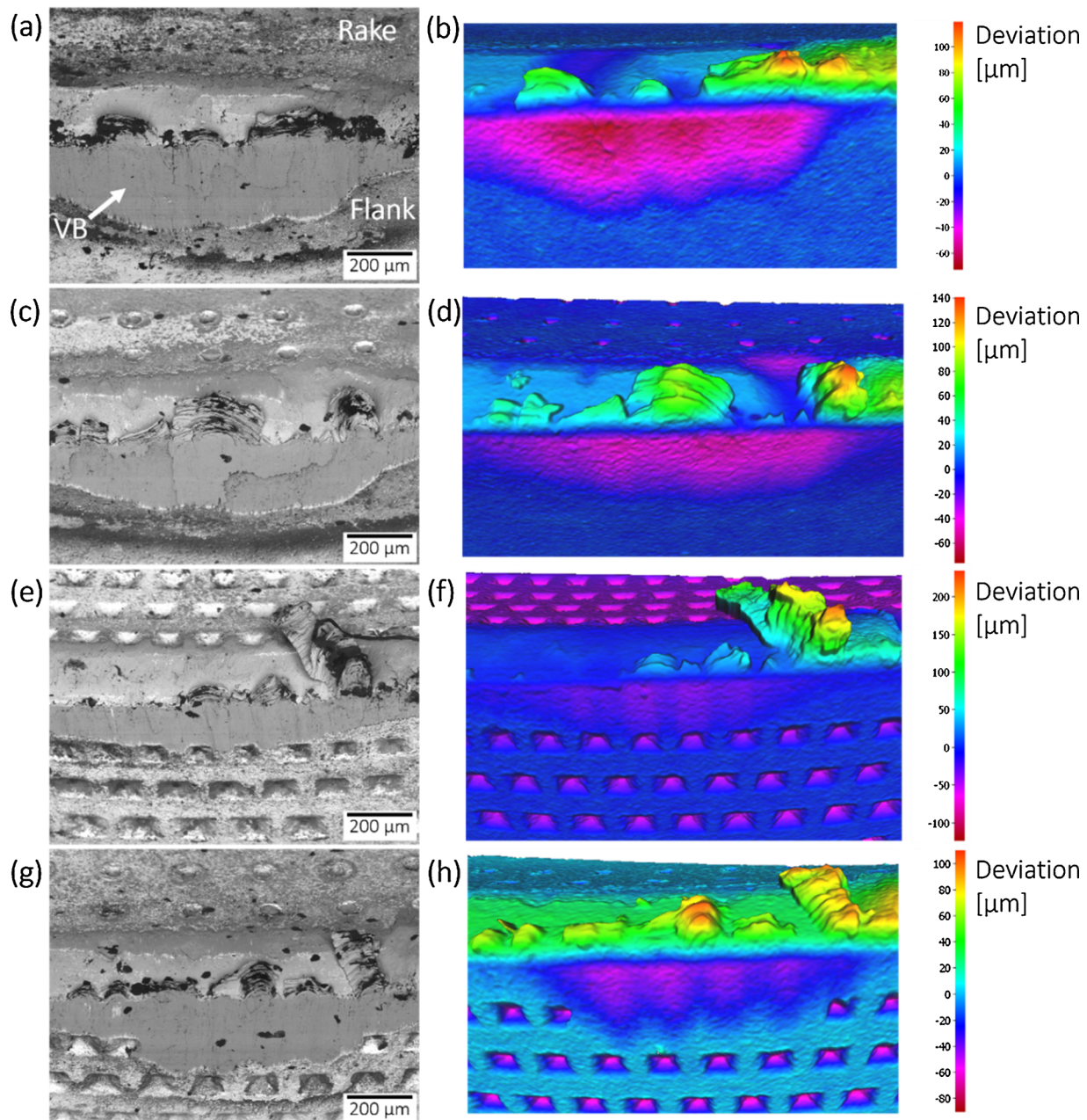
Fig. 13. Cutting edges after the conducted tests imaged by SEM (left column) and 3D topography scans (right column): (a), (b) regular insert; (c), (d) Gen 0 insert; (e), (f) Gen I insert; (g), (h) Gen I+ insert. The topography scans are presented as the geometrical deviation from an unworn insert.
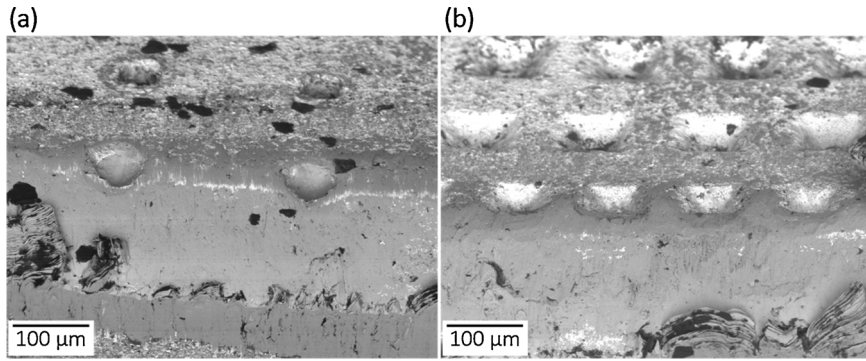
Fig. 14. SEM micrographs of the first rows of patterns on the rake faces: (a) Gen I+ insert; (b) Gen I insert.
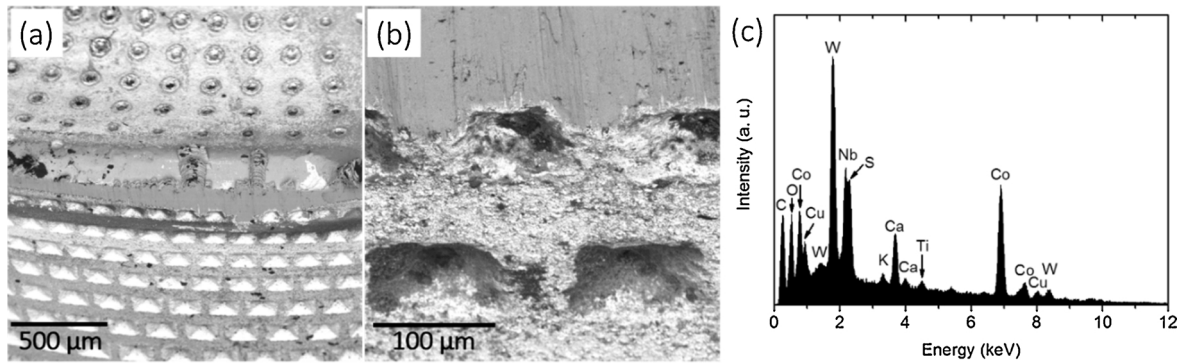

Fig. 15. Layers of burned coolant found on worn inserts: (a), (b) SEM images of worn cutting edges of Gen I+ inserts with burned layers (black) below flank wear land; (c) example of an EDX spectrum of a burned layer found on a worn regular insert.

depth of characteristic X-rays (~1 μm). Jäger et al. [16] reported similar layers below the flank wear lands of inserts used for machining Alloy 718 under influence of high-pressure cooling. The authors linked the adhesion layers to the coolant. Hence, the generation of high temperatures during machining of superalloys can lead to boiling of the cutting fluid once it comes in contact with the tool surface. The dark adhesion layer is therefore likely to be residues/precipitates of the coolant. In that context it should be noted that the presence of coolant residues inside the first rows of indents on the flank face, see Fig. 15(b), suggests that the coolant was able to reach the first row of surface textures.

4.4. Chip thickness and morphology

Investigation of chip morphology and chip thickness was done to understand the effect of cutting tool micro structuring during machining. The chips were collected after each experiment and the chip thickness was measured. The measurement was performed exactly on the half of the chip width. The average chip thickness and standard deviation were evaluated for fifteen chips from every cutting condition for all the tools and their corresponding repetitions. It has to be taken into account that the round shape of the insert leads to a varying undeformed chip thickness (t_0) along the cutting edge. The cutting edge angle (κ_r) as well as maximum undeformed chip thickness (t_{0max}) depends on the depth of cut (a_p) as shown in Fig. 16.

The calculation of the shear angle, φ, is of vital importance to understand the changes in the primary shear zone in correspondence to texturing of the cutting tool. The shear plane angle was calculated from the measured average chip thickness, t_1, and average undeformed chip thickness, t_0, based on the chip thickness ratio, r, and the rake angle, α, see the Eqs. (2) and (3).

$$r = \frac{t_0}{t_1} \tag{2}$$

$$\tan\varnothing = \frac{r \cdot \cos\alpha}{1 - r \cdot \sin\alpha} \tag{3}$$

Fig. 17 shows the measured average chip thickness for the different tools and corresponding standard deviations in relation to the shear plane angle. The Gen 0 and Gen I+ design decreased the shear angle as compared to the regular and Gen I tool. Nevertheless, the drop is relatively small, about 7% in comparison to the regular tool.

The workpiece material was adhered to the rake face of the tools at varying proportions. This is likely due to the coolant interaction on the surface leading to varying the heat dissipation rate forming build up materials as shown in Figs. 13 and 14. Thus, the adhered material influences the tool-chip friction and sliding condition between the chip and textures. For further analysis, the chip back sides, which were in contact with the rake face during machining, were investigated by LOM and SEM. Fig. 18 shows images of a chip for each investigated tool type.

Chips from regular inserts have a smooth surface on the back side. The surface is without any significant mark caused by adhered material;
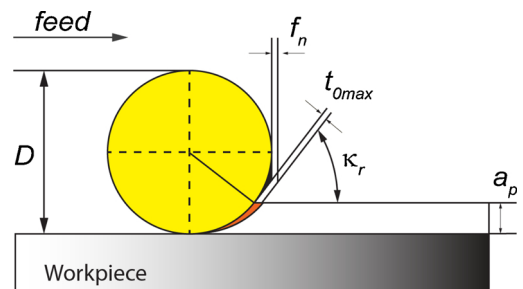

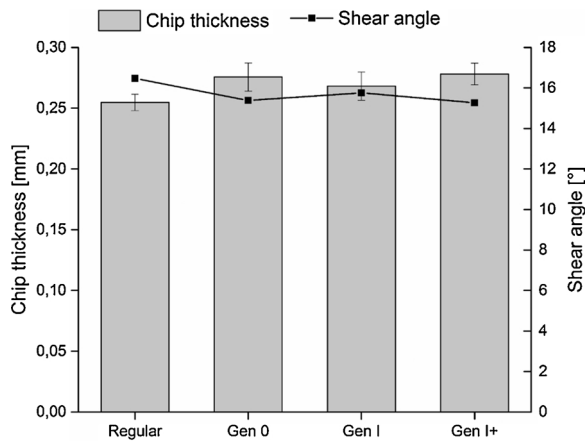**Fig. 16.** Round insert varying chip thickness and entry angle.

Fig. 17. Measured Chip thickness for all insert types and corresponding shear plane angle.

see Fig. 18(a). In contrast, imprints of the textures were found for chips produced with Gen 0 and Gen I+ insert, Fig. 18(b) and (d). The SEM analysis showed that the smoothness on the chip back side is affected by a rake face structure placed in the area of the tool-chip contact. The regular and Gen I inserts generated smooth surfaces. The Gen 0 and Gen I+ inserts with the cylindrical rake face structure created series of linear marks parallel to the direction of chip movement. This shows that the smoothness of the back side of the chip is significantly affected by the rake face structure placed close to the cutting edge in the area of tool-chip contact.

A more detailed view of the chip produced by the Gen I+ insert is shown in Fig. 19. The series of protrusions on the back side of the chip is generated as a consequence of the missing tool material due to the dimples on the tool. In addition, microgrooves were observed close to the protrusion shape. The protrusion's average width was measured to be 86 μm. Hence, it is about 10% larger than the real diameter of the

dimple. The larger width of the protrusion is caused by the wear of the dimple edge during machining and by the not ideally circular shape of the dimple. The pitch of two neighbouring protrusions on the chip is 235 μm in average. This distance is about 6% larger than the real distance of the dimples. The deviation is caused by the non-uniform protrusions generated along the cutting edge owing to the non-uniform chip thickness. To some extent, the deviation can also be attributed to the accuracy of the distance measurement by means of the post-process image analysis.

The detailed observation of chips showed the protrusion is the imprint of the dimple. This confirms that the Gen I+ insert affects tool-chip condition, material adhesion as well as friction condition on the rake face. The highest rate of adhered workpiece material was found on the rake face with cylindrical indents as shown in Fig. 14(a). Similar findings were reported by Xie et al. [18], who showed that the chip thickness increased with textured tools as compared with traditional tools. However, the chips of Ti-6Al-4 V had groove marks, and grooved tools led to a lower cutting force.

Alloy 718 has significantly lower thermal conductivity than sintered carbide, which leads to less amount of heat transferred to the cutting tool during machining. The theoretical chip contact area of Gen I+ inserts as illustrated in Fig. 10(b) can be correlated to the filling of textures with material, see Fig. 12(h). This in turn created grooves on the chip back side as can be seen in Fig. 19. This suggests that the chip "interacts" with the first row of texture during cutting. Thus, they have a positive influence on the tool-chip friction, and filling material in the dimples led to a lowered flank wear.

5. Conclusion

The main intention of the work was to study the performance of different tool textures in terms of the wear behaviour, wear resistance and tool life in machining Alloy 718. The following conclusions were made from the investigation.
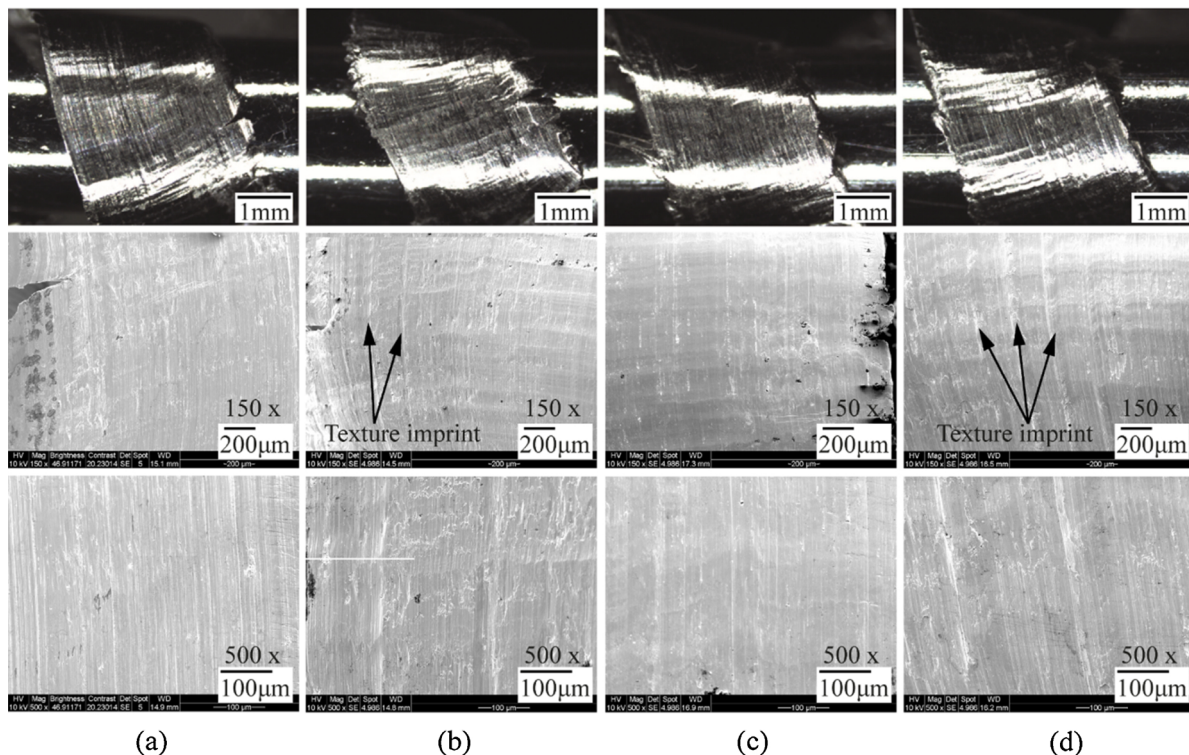

(a)   (b)   (c)   (d)

Fig. 18. Surface morphology of the back side of chips from different tools: (a) regular, (b) Gen 0, (c) Gen I, (d) Gen I+. The first row from top, micrographs is from a light optical microscope; second and third row are SEM micrographs at higher magnifications.
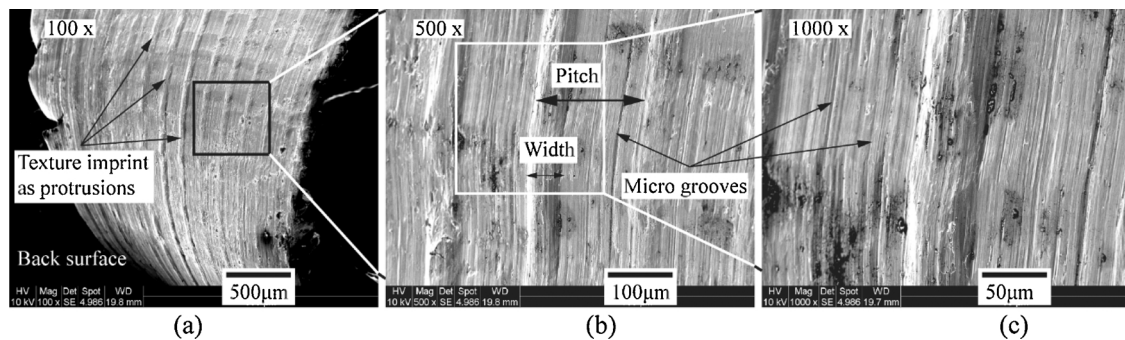
Fig. 19. The SEM micrograph of chip back surface produced from Gen I+ tool: (a) Showing the texture imprints as protrusions (b) and (c) at higher magnification.

1 Neither notch nor crater wear was observed on any of the cutting tools.
2 Cylindrical dimples on the rake face of Gen 0 and Gen I+ were in contact with the chip, leaving protrusion marks on the chip backsides.
3 The textured tools did not have a significant influence on the tool-chip contact area.
4 Varying levels of material adhesion was found on all the tools. Filling of the textures was found on Gen 0 and Gen I+ inserts. Nevertheless, this behaviour did not influence the cutting process negatively.
5 Gen 0 and Gen I+ texture design on the rake face close to the cutting edge did not weaken the mechanical strength of the insert.
6 The Gen I+ insert had better wear resistance, which led to increased tool life by approximately 30% compared to the regular insert.

Based on the obtained results, textured tool has improved the tool performance in machining Alloy 718. Surface featuring on the tool can be identified as the emerging development in the field of cutting tool designs (next generation cutting tools). At the same time, is important to further continue the research in optimizing the design in accordance with the industrial/consumer requirements.

Conflicts of interest

The authors declare no conflict of interests. The funding agency had no role in the experiments, analyses or interpretation of data and in the decision to publish the results.

Acknowledgements

References

[1] Paulonis DF, Schirra JJ. Alloy 718 at Pratt & Whitney: historical perspective and future challenges. 2001. p. 13–23.
[2] Ezugwu EO, Bonney J, Yamane Y. An overview of the machinability of aeroengine alloys. J Mater Process Technol 2003;134(March (2)):233–53.
[3] Rahim E, Warap N, Mohid Z. Thermal-assisted machining of nickel-based alloy. In: Aliofkhazraei M, editor. Superalloys. InTech; 2015.
[4] Pigott RJS, Colwell AT. Hi-jet system for increasing tool life. SAE Tech. Pap.; 1952.
[5] Kawasegi N, Sugimori H, Morimoto H, Morita N, Hori I. Development of cutting tools with microscale and nanoscale textures to improve frictional behavior. Precis Eng 2009;33(July (3)):248–54.
[6] Lei S, Devarajan S, Chang Z. A study of micropool lubricated cutting tool in machining of mild steel. J Mater Process Technol 2009;209(February (3)):1612–20.
[7] Enomoto T, Sugihara T, Yukinaga S, Hirose K, Satake U. Highly wear-resistant cutting tools with textured surfaces in steel cutting. CIRP Ann—Manuf Technol 2012;61(1):571–4.
[8] Sugihara T, Enomoto T. Improving anti-adhesion in aluminum alloy cutting by micro stripe texture. Precis Eng 2012;36(April (2)):229–37.
[9] Obikawa T, Kamio A, Takaoka H, Osada A. Micro-texture at the coated tool face for high performance cutting. Int J Mach Tools Manuf 2011;51(December (12)):966–72.
[10] Koshy P, Tovey J. Performance of electrical discharge textured cutting tools. CIRP Ann—Manuf Technol 2011;60(1):153–6.
[11] Ma J, Duong NH, Lei S. 3D numerical investigation of the performance of micro-groove textured cutting tool in dry machining of Ti-6Al-4V. Int J Adv Manuf Technol 2015;79(July (5–8)):1313–23.
[12] Fang Z, Obikawa T. Cooling performance of micro-texture at the tool flank face under high pressure jet coolant assistance. Precis Eng 2017;49(July):41–51.
[13] "Sandvik Coromant. Application Guide - Heat resistant super alloys." Sandvik Coromant, Aug-2010.
[14] Tamil Alagan N, Beno T, Hoier P, Klement U, Wretland A. Influence of surface features for increased heat dissipation on tool wear. Materials 2018;11(April (5)):664.
[15] ISO 3685:1993. Tool-life testing with single-point turning tools-ISO 3685:1993. 2011.
[16] Jäger H, Alagan NT, Holmberg J, Beno T, Wretland A. EDS analysis of flank wear and surface integrity in machining of alloy 718 with forced coolant application. Procedia CIRP 2016;45:271–4.
[17] Hoier P, Klement U, Tamil Alagan N, Beno T, Wretland A. Flank wear characteristics of WC-Co tools when turning alloy 718 with high-pressure coolant supply. J Manuf Process 2017;30(December):116–23.
[18] Xie J, Luo M-J, He J-L, Liu X-R, Tan T-W. Micro-grinding of micro-groove array on tool rake surface for dry cutting of titanium alloy. Int J Precis Eng Manuf 2012;13(October (10)):1845–52.